before freezing on their way to the surface. The symmetrical mineralogical layering of the pyroxenite layers, which has been taken as indicating a magmatic fractionation sequence (*25*), is also consistent with melt-mediated mineral reactions at length scales of tens of centimeters. For small fractions of melt, the oxygen isotope composition of the peridotite would be preserved, but the Hf isotopic signature would not. It would instead be dominated by the radiogenic melt component. The extreme Nd and Hf isotopic properties of many peridotites and pyroxenites require that truly primary melts never get sampled as basalts.

The solution to the origin-of-basalt dilemma (*10, 31*), which suggests either isobaric melting of a heterogeneous pyroxenite/peridotite source or polybaric melting of a more homogeneous peridotite source, may rather be a combination of these two scenarios. A "normal" piece of mantle may be dominated by coexisting pyroxenite residues and peridotites that were contaminated by the pervasive circulation of pyroxenite melts. Although the "marble cake" mantle is a seminal concept, the present isotopic evidence suggests that the original ingredients became somewhat mixed up, or even preferentially lost, to the point that the original recipe has become difficult to decipher. Geochemical heterogeneities therefore should be handled as active rather than as passive Lagrangian tracers by convection models.

The lower Lu/Hf ratio of oceanic basalts with respect to the time-integrated ratio deduced for the mantle source of the basalts from their Hf isotope systematics is an apparent inconsistency (dubbed the "Hf paradox"), which Salters and Hart (*2*) explained by the presence of garnet during melting. This model has recently been challenged by Blundy *et al.* (*4*), who redetermined the partition coefficients of clinopyroxene and melt and found that, at 1.5 GPa and for small degrees of melting (1%), Lu, Hf, Sm, and Nd are five times more compatible than currently thought. They combined these data with results on garnet (*33*) to create a critical partitioning parameter (CPP) $(D_{Sm}/D_{Nd})/(D_{Lu}/D_{Hf})$, where D stands for the mineral/melt partition coefficients, which they use to argue that the Nd-Hf isotope systematics of MORBs do not require residual garnet during melting. Although garnet pyroxenites cannot be used to infer the CPP of each mineral, ratios of CPP for garnet and clinopyroxene at mantle conditions may be inferred from mineral/mineral partitioning, provided that subsolidus reequilibration is not extreme. In our samples, which were equilibrated at pressures of at least 1.5 GPa (*13*), which is close to the experimental conditions of Blundy *et al.* (*4*), the Lu/Hf fractionation between garnet (ga) and clinopyroxene (cpx) is strong with $(D_{Lu}/D_{Hf})_{ga}/(D_{Lu}/D_{Hf})_{cpx}$ in the range of 55 to 150. These values can be combined with the $(D_{Sm}/D_{Nd})_{ga}/(D_{Sm}/D_{Nd})_{cpx}$ value of ~5, which was observed in our study and in (*16*), to produce a CPP_{ga}/CPP_{cpx} ratio that is in the range of 0.03 to 0.1, which is well below the range of 0.8 to 2.1 deduced from the experimental data (*4, 33*). Part of the reason for this inconsistency may be that the experimental partition coefficients have not been obtained on a molten assemblage with garnet and clinopyroxene coexisting in the residue. We nevertheless consider that the compatibility of Sm, Nd, Lu, and Hf in clinopyroxene may have been overestimated by previous experiments and that residual garnet in the source of basalts still represents the best answer to the Hf paradox.

References and Notes

1. C. J. Allègre and D. L. Turcotte, *Nature* **323**, 123 (1986).
2. V. J. M. Salters and S. R. Hart, *ibid.* **342**, 420 (1989).
3. T. Z. LaTourrette, A. K. Kennedy, G. J. Wasserburg, *Science* **261**, 739 (1993).
4. J. D. Blundy, J. A. C. Robinson, B. J. Wood, *Earth Planet. Sci. Lett.* **160**, 493 (1998).
5. D. A. Wood, *Geology* **7**, 499 (1979).
6. A. Zindler, H. Staudigel, R. Batiza, *Earth Planet. Sci. Lett.* **70**, 175 (1984).
7. M. Roy-Barman and C. J. Allègre, *ibid.* **129**, 145 (1995).
8. C. C. Lundstrom, Q. Williams, J. B. Gill, *ibid.* **157**, 151 (1998).
9. D. McKenzie and R. K. O'Nions, *J. Petrol.* **32**, 1021 (1991).
10. B. Bourdon, A. Zindler, T. Elliott, C. H. Langmuir, *Nature* **384**, 231 (1996).
11. V. J. M. Salters and A. Zindler, *Earth Planet. Sci. Lett.* **129**, 13 (1995).
12. V. V. Slodkevitch, *Mineral. Soc. U.S.S.R.* **1**, 13 (1982).
13. J. Kornprobst, *Contrib. Mineral. Petrol.* **23**, 283 (1969).
14. ———, *Notes Serv. Geol. Maroc* **251**, 1 (1974).
15. K. Gjata, J. Kornprobst, A. Kodra, D. Briot, F. Pineau, *Bull. Soc. Geol. Fr.* **163**, 469 (1992).
16. N. Kumar, L. Reisberg, A. Zindler, *Geochim. Cosmochim. Acta* **60**, 1429 (1996).
17. D. G. Pearson, G. R. Davies, P. H. Nixon, *J. Petrol.* **34**, 125 (1993).
18. T. P. Loomis, *Am. J. Sci.* **275**, 1 (1975).
19. S. Duchêne *et al.*, *Nature* **387**, 586 (1997).
20. Y. Ricard and C. Vigny, *J. Geophys. Res.* **94**, 17543 (1989).
21. P. Vergely, A. Dimo, P. Monié, *C. R. Acad. Sci. Paris* **326**, 717 (1998).
22. References for Hf isotope data in oceanic basalts can be obtained from J. Blichert-Toft upon request.
23. L. Reisberg and A. Zindler, *Earth Planet. Sci. Lett.* **81**, 29 (1986/1987).
24. ———, E. Jagoutz, *ibid.* **96**, 161 (1989).
25. D. G. Pearson, G. R. Davies, P. H. Nixon, P. B. Greenwood, D. P. Mattey, *ibid.* **102**, 289 (1991).
26. A. Zindler and S. Hart, *Annu. Rev. Earth Planet. Sci.* **14**, 493 (1986).
27. M. Javoy, in *Orogenic Mafic and Ultramafic Association*, vol. 272 of *Colloques Internationaux du CNRS*, C. J. Allègre and J. Aubouin, Eds. (Editions du CNRS, Paris, 1980), pp. 279–287.
28. J. C. Lassiter, E. H. Hauri, P. W. Reiners, M. O. Garcia, *Mineral. Mag.* **62A**, 856 (1998).
29. M. Loubet and C. J. Allègre, *Nature* **298**, 809 (1982).
30. J. Kornprobst, M. Piboule, M. Roden, A. Tabit, *J. Petrol.* **31**, 717 (1990).
31. M. M. Hirschmann and E. M. Stolper, *Contrib. Mineral. Petrol.* **124**, 185 (1996).
32. E. H. Hauri, *Earth Planet. Sci. Lett.* **153**, 1 (1997).
33. W. van Westrenen, J. Blundy, B. Wood, *Am. Mineral.*, in press.
34. J. Blichert-Toft, C. Chauvel, F. Albarède, *Contrib. Mineral. Petrol.* **127**, 248 (1997).

35. We are grateful to P. Télouk for keeping the Plasma 54 inductively coupled plasma mass spectrometer in optimum working condition. We thank two anonymous reviewers for helpful comments.

22 October 1998; accepted 20 January 1999

Seismic Evidence for a Detached Indian Lithospheric Mantle Beneath Tibet

G. Kosarev,[1] R. Kind,[2,3]* S. V. Sobolev,[2] X. Yuan,[2] W. Hanka,[2] S. Oreshin[1]

P-to-*S* converted teleseismic waves recorded by temporary broadband networks across Tibet show a north-dipping interface that begins 50 kilometers north of the Zangbo suture at the depth of the Moho (80 kilometers) and extends to a depth of 200 kilometers beneath the Bangong suture. Under northern Tibet a segmented south-dipping structure was imaged. These observations suggest a different form of detachment of the Indian and Asian lithospheric mantles caused by differences in their composition and buoyancy.

Although the altitude of the Tibetan Plateau is uniform, physical properties of the lithosphere (crust and upper mantle) such as velocity and density are different in northern and southern Tibet (*1–16*), suggesting fundamental differences in the origin of the lithosphere in these two regions. In the upper mantle in northern Tibet, the propagation of S_n waves is inefficient (*8, 9*), P_n velocities are slow (*5*), and there exists a low-velocity body (*16*). Together with evidence for a higher Poisson ratio in the crust of northern Tibet (*2*) and the presence of volcanic activity (*17*), these data suggest

[1]Institute of the Physics of the Earth, Russian Academy of Sciences, B. Gruzinskaya 10, 128810 Moscow, Russia. [2]GeoForschungsZentrum Potsdam, Telegrafenberg, 14473 Potsdam, Germany. [3]Freie Universität Berlin, Geophysik, Malteser Strasse 74-100, 12249 Berlin, Germany.

*To whom correspondence should be addressed. E-mail: kind@gfz-potsdam.de

a higher temperature for the crust and mantle in northern Tibet (*2–4*). According to Owens and Zandt (*2*), these observations indicate that the cold Indian lithospheric mantle has underthrust the Asian crust to the Bangong suture and is truncated there by a steeply dipping subduction zone, whereas northern Tibet has a thin lithosphere and a hot, partially molten crust. However, the geometry of the underthrusting or subducting Indian lithospheric mantle is not well constrained because no deep earthquakes have been recorded (*18*) and no other direct seismic observations have been available.

To infer structures in the upper mantle that could be related to subduction or other processes, we reexamined data from the 1991 to 1992 Sino-American PASSCAL experiment (*2, 3, 5, 7, 8, 19–21*) and the international 1994 INDEPTH II/GEDEPTH experiment (*12–14, 22*), which have so far mainly been analyzed to model crustal structures. The data we used consisted of 353 teleseismic receiver functions (RFs) (*22–25*) from INDEPTH II/GEDEPTH and 406 RFs from PASSCAL (Fig. 1).

In a modification of the RF technique (*22, 24*), the *P*-to-*S* converted teleseismic phases (which are time series) (Fig. 2) are migrated into spatial images of the lithosphere and upper mantle beneath the receiver array (*25*). For this purpose a reference velocity model (*26*) was divided into 4 km by 4 km (horizontally) by 2 km (vertically) boxes, and the RFs were traced back from the receiver to the source through these boxes. All RFs (originating from different sources and recorded at different stations) passing through one box were averaged.

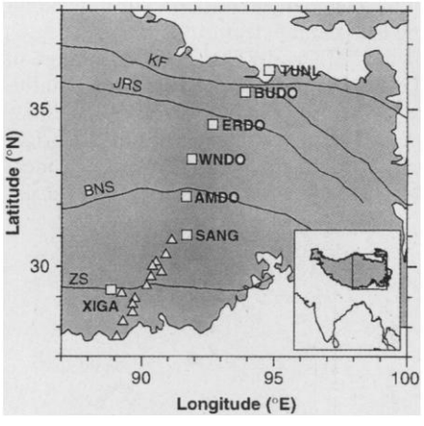

Fig. 1. Location map of the seismic stations of the international passive source experiments INDEPTH II/GEDEPTH (triangles, 1994) and PASSCAL (squares, 1991 to 1992). The heavy contour line marks the 4-km altitude that defines the approximate physiographic boundary of the Tibetan Plateau. ZS, Zangbo suture; BNS, Bangong suture; JRS, Jinsha River suture; KF, Kunlun fault.

The Moho is seen across the entire plateau (Fig. 3). It dips smoothly to the north from the southern end of the profile to just north of the Zangbo suture where it reaches a depth of about 80 km. Further to the north it returns to shallower depths. The images of the 410- and 660-km discontinuities also smoothly dip to the north and are parallel. The northward dip may be an artifact caused by a northward decrease in the *S*-wave velocity in the upper mantle above 410-km depth, thus supporting earlier observations (*16*). We also see a flat, wide, diffuse band of energy between a depth of 200 and 300 km, which is caused by multiple reflections inside the crust. Multiple reflections are frequently a problem in RF analysis (as in seismic reflection studies) and must be considered carefully (*27*).

A north-dipping *P*-to-*S* conversion boundary (*27*), hereafter called the Zangbo conversion boundary (ZCB), begins close to the Zangbo suture. The amplitude of the converted wave at this boundary is about 4 to 6% that of the direct *P* wave. For the observed wave period of 3 s, this can be modeled by an *S*-wave velocity increase of 6 to 8% over a depth interval of ≤20 km using the reflectivity method (*28*). Such a velocity change may be explained by a temperature contrast of 500° to 700°C [considering the effects of anelasticity and chemical reactions (*29*)] together with chemical differences (a higher Mg content in the cratonic mantle). This suggests that the ZCB may separate the relatively cold and chemically depleted cratonic lithospheric mantle of India with a temperature of 600° to 800°C at its top from the lower lithosphere of Asia with a temperature of

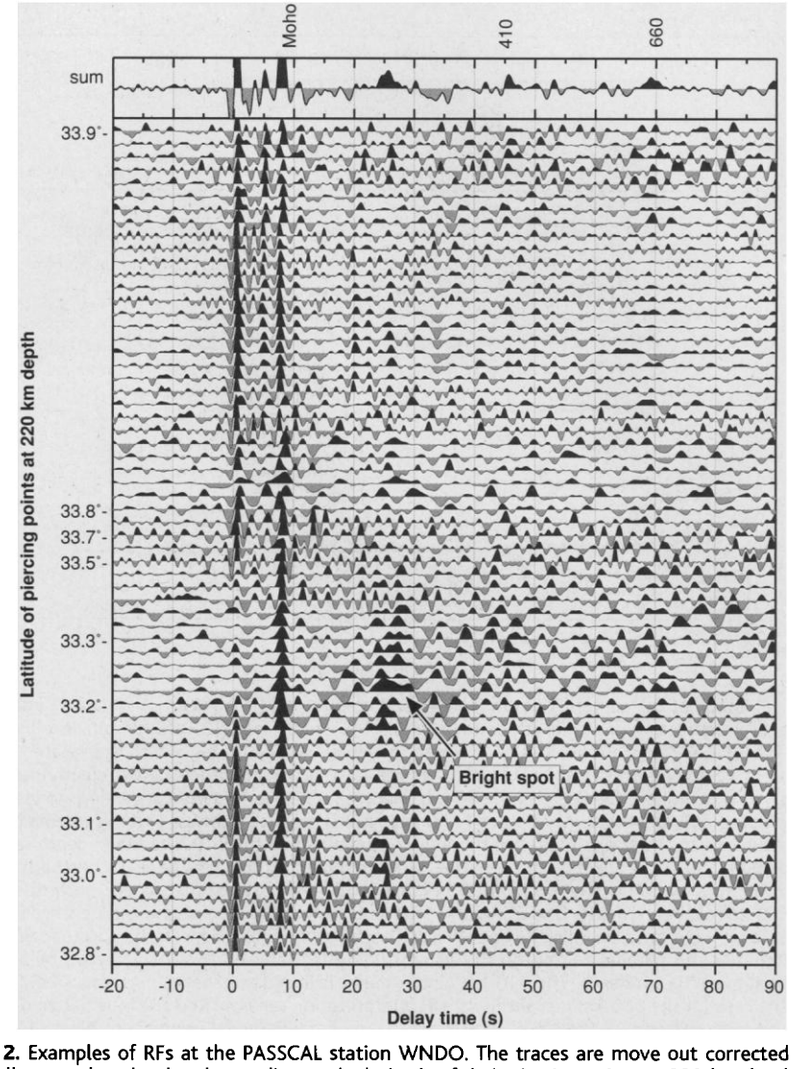

Fig. 2. Examples of RFs at the PASSCAL station WNDO. The traces are move out corrected (*34*), equally spaced, and ordered according to the latitude of their piercing points at 220-km depth. The Moho is seen on almost all the traces. The 410- and 660-km discontinuities are seen in the summation trace at the top of the figure. Zero time is the *P*-wave arrival time. The bright spot is also marked in the migrated section in Fig. 3.

1100° to 1300°C just above the Indian mantle (*30*) (Fig. 3B). There are at least two other independent sources of evidence that support our model. Teleseismic travel time tomography in northern Tibet along a line that almost coincides with our line reveals a *P*-wave velocity contrast of about 5% at a depth of 200 to 250 km (*16*). If this velocity difference was between the normal asthenosphere and a plume (*16*) the corresponding excess temperature of the plume would be more than 400°C (*29*). Most of the observed velocity contrast can be explained by a lower temperature and higher Mg content of the Indian lithospheric mantle (Fig. 3B), and the remainder (1 to 2%) by an upwelling of the hot Asian mantle with a temperature excess of 100° to 200°C. Additionally, the joint interpretation of the surface topography and the gravity field in southern Tibet (*10*) suggests a similar model of the Indian mantle lithosphere as does our model.

There is a zone of *P*-to-*S* conversions in northern Tibet that dips to the south [northern conversion zone, NCZ in Fig. 3A (*27*)]. Although the polarity and amplitude of the converted waves at the NCZ and ZCB are similar, these boundaries look different. The ZCB is continuous, whereas the NCZ appears to consist of segments dipping in the opposite direction of the general southern dip of the entire NCZ. The complicated mantle conversions in the north may be due to segments of relatively cold mantle material (700° to 1000°C) within a normal or hot asthenosphere (1300° to 1500°C). The ZCB and NCZ meet at 200- to 250-km depth and 50 to 100 km north of the Bangong suture where an exceptionally bright spot (defined by large amplitudes) is imaged below the station WNDO (Figs. 2 and 3A) (*31*). The piercing points of the converted phases below WNDO form a near continuous north-south band east of the station (Fig. 4). The bright spot is marked by a confined cluster in the center of the piercing points, approximately defining the lateral extent of the merging region of the NCZ and ZCB. The depth range of the bright spot (200 to 250 km) is influenced by crustal multiples, but these likely are not the dominant feature at the bright spot because the Moho conversions there do not show comparable irregularities, in-

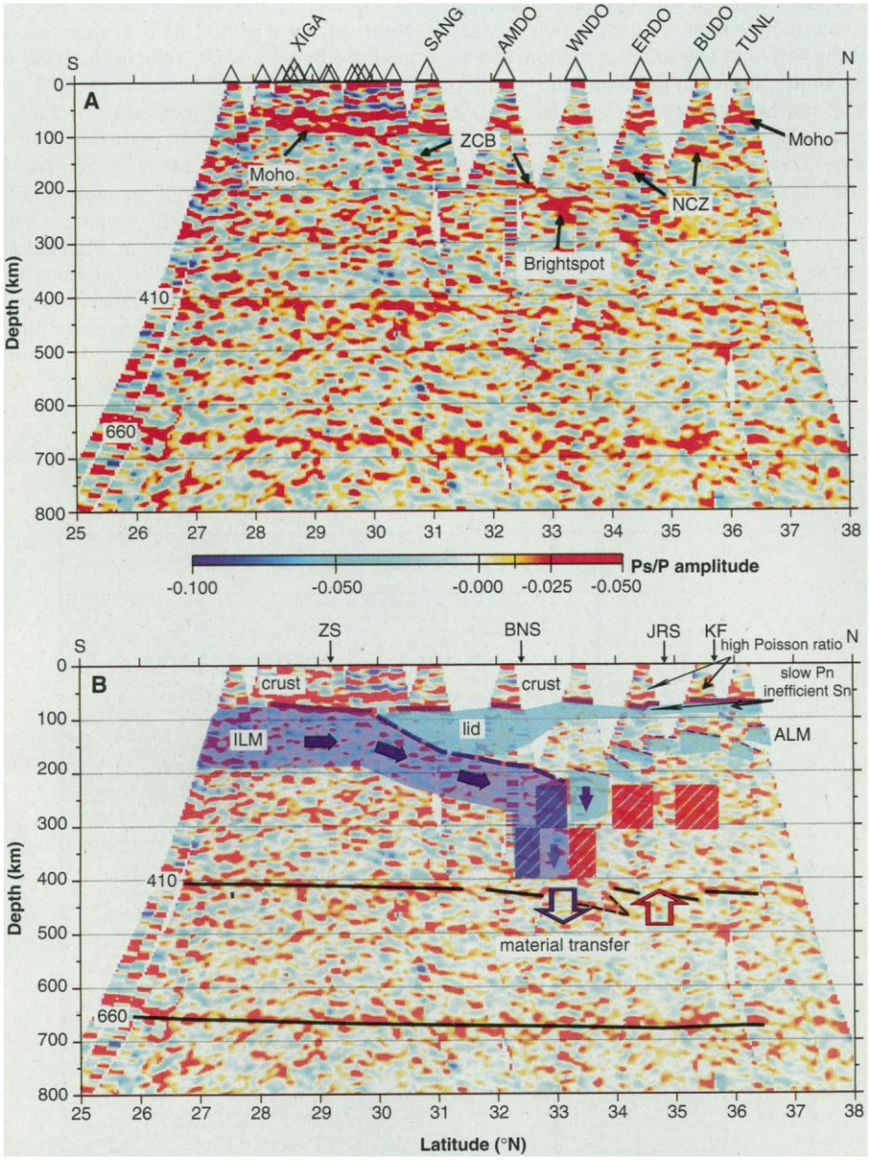

Fig. 3. RF image of the eastern Tibetan Plateau and its interpretation. (**A**) A migrated RF image of the upper mantle showing a north-south profile. The small triangles at the top left indicate INDEPTH II/GEDEPTH stations. Red colors mark positive RF amplitudes, which are related to an increase of velocity with depth, and blue colors mark negative amplitudes. Most clearly seen are images of the Moho, the 410- and 660-km discontinuities, and two conversion zones—the north-dipping ZCB and the south-dipping NCZ. The NCZ is more segmented (with segments having different dips than the entire NCZ) and more discontinuous than the ZCB. The Moho depth reaches its maximum (80 km) beneath southern Tibet and its minimum (60 km) beneath northern Tibet. There is an interruption in the Moho at 30°N latitude (50 km north of the Zangbo suture), where it reaches its maximum depth. The ZCB starts from the Moho at this point and can be traced down to a depth of ~250 km below the station WNDO (bright spot). The images of the 410- and 660-km discontinuities dip parallel to the north, which may reflect the northward decrease of *S*-wave velocity above 410-km depth. The 410-km discontinuity is irregular beneath northern Tibet, which is not the case for the 660-km discontinuity. (**B**) Interpretation cartoon. Red and blue hatched boxes show the main features of the travel time *P*-wave tomographic model in northern Tibet (*16*). The velocity contrast between high-speed blocks (blue) and low-speed blocks (red) is about 5%. The ZCB is interpreted as the boundary between the cold and depleted lithospheric mantle of India (ILM, partially transparent dark blue) and the Asian lithospheric mantle (ALM, partially transparent light blue). The NCZ is interpreted as an image of the Asian lithospheric mantle in the process of destruction and subduction.

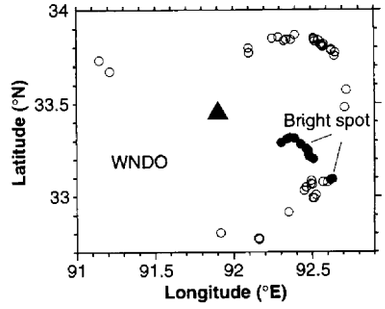

Fig. 4. Location of piercing points of *P*-to-*S* converted phases at 220-km depth of the traces in Fig. 2.

dicating a more homogeneous crust than mantle at a depth of 200 to 250 km (Fig. 2).

There are also differences in the character of the *P*-to-*S* conversions at the 410-km discontinuity beneath southern and northern Tibet. Northern Tibet is underlain by an irregular 410-km discontinuity. One possible explanation for the complicated character of the 410-km discontinuity beneath northern Tibet could be the presence of mass transfer through the boundary there.

Our data support previous observations that indicate that the fundamental differences between the crustal and mantle structure of southern and northern Tibet may be related to a higher mantle temperature beneath northern Tibet. An explanation for this phenomenon most likely would involve two processes: (i) preservation of a lithosphere thickened by collision in the south (*4*), and (ii) destruction and thinning of the postcollision thick mantle lithosphere in the north (*2*–*6*). The presence of the north-dipping *P*-to-*S* conversion boundary (ZCB) and the previously reported tomographic model (*16*) suggest that the cold Indian lithosphere has underthrust the Asian lithosphere [not just the Asian crust, as suggested in (*2*)] in the south, thus preventing it from being destroyed (Fig. 3B). The zone of strong and complicated conversions in the north (Fig. 3) may indicate an ongoing process of destruction and subduction of the Asian lithospheric mantle, which in this case appears to be more complicated than simple convective lithospheric thinning in a viscous media (*4*). The complicated character of the 410-km discontinuity in the north and the hot mantle material imaged by seismic tomography directly above this discontinuity support the idea of extensive mass transfer between the upper mantle and the transition zone in northern Tibet.

One possible reason for the difference in the detachment styles of Indian and Asian lithospheric mantles displayed in Fig. 3B is a difference in chemical composition of the cratonic mantle lithosphere of India and the relatively young mantle lithosphere of Asia. The former should be buoyant in the normal asthenosphere and thus essentially unsubductable, whereas the latter should be denser than the underlying asthenosphere and thus mechanically unstable (*32*).

Finally, we would like to make some comments concerning the possible nature of the bright spot in central Tibet (Figs. 2, 3, and 4). The striking feature of the bright spot is that it is located exactly in the region where the ZCB and NCZ meet. According to our interpretation of those features, we suggest that the bright spot may be related to the collision of the Indian and Asian lithospheric mantles in central Tibet. The high conversion coefficient at the bright spot (6 to 8%) and the associated large *S*-velocity contrast (more than 10%) cannot be explained by only temperature and chemical differences between the older Indian and Asian lithospheric mantles and the asthenosphere. Therefore other processes, such as extreme strain localization and associated olivine crystals alignment, heating and even melting of the rocks (probably possible only in the presence of fluid at depths of 200 to 250 km), or an increase in the water content of olivine due to the water released from subducted Tethyan lithosphere, may contribute to the *S*-velocity contrast at the bright spot.

References and Notes

1. P. Molnar, *Philos. Trans. R. Soc. London Ser. A* **326**, 33 (1988).
2. T. J. Owens and G. Zandt, *Nature* **387**, 37 (1997).
3. L. Zhu, T. J. Owens, G. E. Randall, *Bull. Seismol. Soc. Am.* **85**, 1531 (1995).
4. P. Molnar, P. England, J. Martinod, *Rev. Geophys.* **31**, 357 (1993).
5. D. E. McNamara, W. R. Walter, T. J. Owens, C. J. Ammon, *J. Geophys. Res.* **102**, 493 (1997).
6. D. Willett and C. Beaumont, *Nature* **369**, 642 (1994).
7. D. E. McNamara, T. J. Owens, P. G. Silver, F. T. Wu, *J. Geophys. Res.* **99**, 13655 (1994).
8. D. E. McNamara, T. J. Owens, W. R. Walter, *ibid.* **100**, 22215 (1995).
9. J. Ni and M. Barazangi, *Geophys. J. R. Astron. Soc.* **72**, 665 (1983).
10. Y. Jin, M. McNutt, Y. Zhu, *J. Geophys. Res.* **101**, 11275 (1996).
11. W. Zhao *et al.*, *Nature* **366**, 557 (1993).
12. K. D. Nelson *et al.*, *Science* **274**, 1684 (1996).
13. R. Kind *et al.*, *ibid.*, p. 1692.
14. L. D. Brown *et al.*, *ibid.*, p. 1688.
15. A. Hirn *et al.*, *Nature* **307**, 25 (1984); A. Hirn *et al.*, *ibid.* **375**, 571 (1995).
16. G. Wittlinger *et al.*, *Earth Planet. Sci. Lett.* **139**, 263 (1996).
17. S. Turner *et al.*, *Nature* **364**, 50 (1993).
18. P. Molnar and W. P. Chen, *J. Geophys. Res.* **88**, 1180 (1983).
19. T. J. Owens, G. E. Randall, F. T. Wu, R. Zeng, *Bull. Seismol. Soc. Am.* **83**, 1959 (1993).
20. R. Zeng, Z. Ding, Q. Wu, *Pure Appl. Geophys.* **145**, 425 (1995).
21. L. Zhao, M. K. Sen, P. Stoffa, C. Frohlich, *Geophys. J. Int.* **125**, 355 (1996).
22. X. Yuan, J. Ni, R. Kind, J. Mechie, E. Sandvol, *J. Geophys. Res.* **102**, 27491 (1997).
23. T. J. Owens, G. Zandt, S. R. Taylor, *ibid.* **89**, 7783 (1984).
24. M. G. Bostock, *Nature* **390**, 392 (1997).
25. C. H. Jones and R. A. Phinney, *J. Geophys. Res.* **103**, 10065 (1998).
26. B. L. N. Kennett and E. R. Engdahl, *Geophys. J. Int.* **105**, 429 (1991).
27. Crustal multiples, which means a *P*-to-*S* conversion plus two additional *P* legs or one *P* and one *S* leg in the crust, are frequently observed and used in inversions of crustal structure [R. Kind, G. L. Kosarev, N. V. Petersen, *Geophys. J. Int.* **121**, 191 (1995)]. They interfere with original conversions from the depth range between 200 and 300 km. Multiples may be identified by their difference in slowness compared with the original conversions; however, this is sometimes difficult to observe. The migration reduces the influence of multiples if sufficient ray coverage is available. The separation of crustal multiples from inclined structures in the mantle is relatively easy if the Moho is not, or only weakly, inclined (as in Tibet) and structures in the mantle are strongly inclined. The ZCB has a north dip of 20°, whereas the Moho above dips south by 2° to 3°, ruling out the possibility of the ZCB being a crustal multiple. The NCZ dips south by ~25°, whereas *PP* and *PS* crustal multiples would have dips of 8° to 9°. This also rules out the possibility that the NCZ could be a Moho multiple.
28. R. Kind, *J. Geophys.* **58**, 146 (1985).
29. S. V. Sobolev *et al.*, *Earth Planet. Sci. Lett.* **139**, 147 (1996).
30. Other factors such as remnants of the lower crust subducted along with the Indian lithospheric mantle or a lattice-preferred orientation of olivine crystals in the interplate shear zone may also contribute to the observed velocity contrast at the ZCB. However, this is difficult to quantify until more data about the conversion coefficient and thickness of the ZCB is available.
31. Although north of 30.5° latitude we have data only from the relatively few stations of the PASSCAL experiment, there is practically no difference between the signal-to-noise ratio of the averaged converted phases and that of the more numerous data from the INDEPTH II/GEDEPTH experiment in the south. The averaged amplitudes over the entire profile are at the Moho ≥10% of the incident *P* wave; at the bright spot 6 to 8%; and at the ZCB, NCZ, 410-, and 660-km discontinuities 4 to 6%. The overall noise level is about 2 to 4%.
32. Cratonic upper mantle, which is documented by xenolith samples found in kimberlite pipes all over the world [N. V. Sobolev, *Deep Seated Inclusions in Kimberlites and the Problem of the Composition of the Upper Mantle* (American Geophysical Union, Washington, DC, 1977)], was shown to be deficient in Fe (enriched in Mg) relative to the young continental lithospheric mantle and oceanic mantle [F. R. Boyd *et al.*, *Contrib. Mineral. Petrol.* **128**, 228 (1997), and references therein]. A high Mg content of cratonic mantle peridotite makes it significantly less dense than younger lithospheric mantle at the same temperature, and this has important tectonic consequences (*33*). Using a petrophysical modeling technique [S.V. Sobolev and A. Yu. Babeyko, *Surv. Geophys.* **15**, 515 (1994)] and the major element compositions of mantle xenolith samples from cratons [S. Bernstein, P. B. Kelemen, C. K. Brooks, *Earth Planet. Sci. Lett.* **154**, 221 (1998), and references therein] and young continental lithospheres [H. Downes, in *Mantle Xenoliths*, P. H. Nixon, Ed. (Wiley, Chichester, UK, 1987), p. 125; F. Werling and R. Altherr, *Tectonophysics* **275**, 119 (1997)], we estimate the compositionally induced density difference between cratonic and young lithospheric mantles to be ~0.05 g/cm^3. Although a lower temperature of the cratonic lithosphere (by 200° to 300°C) may reduce this difference (to 0.02 to 0.03 g/cm^3), a cratonic lithospheric mantle is still much more buoyant in the asthenosphere than a young lithospheric mantle.
33. T. H. Jordan, *Nature* **274**, 544 (1978).
34. The travel time curves of the *P* phase and the *P*-to-*S* converted phases have different slopes. To make these travel time curves parallel, we compressed the time scale at distances smaller than 67° epicentral distance and expanded it at larger distances. The time scale is therefore only valid for 67° epicentral distance (*22*, *24*). Such a move out correction is common procedure in steep-angle reflection experiments.

35. Supported by the German Bundesministerium für Bildung und Forschung. The INDEPTH II/GEDEPTH experiment was supported by the GeoForschungsZentrum Potsdam, the Deutsche Forschungsgemeinschaft, the U.S. National Science Foundation, and the Chinese Academy of Geological Sciences. Data from the Tibet PASSCAL experiment were collected in a joint project between the University of South California (T. Owens and G. Randall), State University of New York–Binghamton (F. Wu), and the research group of R. Zeng, Institute of Geophysics, State Seismological Bureau, China. We thank X. Li for computational support, and C. Estabrook, G. Bock, and D. Harlov for carefully reading the manuscript.

4 September 1998; accepted 15 January 1999